

The USP1/UAF1 Complex Promotes Double-Strand Break Repair through Homologous Recombination^{∇†}

Junko Murai,^{1,2} Kailin Yang,² Donniphat Dejsuphong,² Kouji Hirota,¹
Shunichi Takeda,¹ and Alan D. D'Andrea^{2*}

*Department of Radiation Genetics, Kyoto University Graduate School of Medicine, Yoshida Konoe, Sakyo-ku, Kyoto 606-8501, Japan,¹ and
Department of Radiation Oncology, Dana-Farber Cancer Institute, Harvard Medical School, Boston, Massachusetts 02115²*

Received 13 January 2011/Returned for modification 7 February 2011/Accepted 29 March 2011

Protein ubiquitination plays a key role in the regulation of a variety of DNA repair mechanisms. Protein ubiquitination is controlled by the coordinate activity of ubiquitin ligases and deubiquitinating enzymes (DUBs). The deubiquitinating enzyme USP1 regulates DNA repair and the Fanconi anemia pathway through its association with its WD40 binding partner, UAF1, and through its deubiquitination of two critical DNA repair proteins, FANCD2-Ub and PCNA-Ub. To investigate the function of USP1 and UAF1, we generated *USP1*^{-/-}, *UAF1*^{-/-}, and *USP1*^{-/-} *UAF1*^{-/-} chicken DT40 cell clones. These three clones showed similar sensitivities to chemical cross-linking agents, to a topoisomerase poison, camptothecin, and to an inhibitor of poly(ADP-ribose) polymerase (PARP), indicating that the USP1/UAF1 complex is a regulator of the cellular response to DNA damage. The hypersensitivity to both camptothecin and a PARP inhibitor suggests that the USP1/UAF1 complex promotes homologous recombination (HR)-mediated double-strand break (DSB) repair. To gain insight into the mechanism of the USP1/UAF1 complex in HR, we inactivated the nonhomologous end-joining (NHEJ) pathway in UAF1-deficient cells. Disruption of NHEJ in UAF1-deficient cells restored cellular resistance to camptothecin and the PARP inhibitor. Our results indicate that the USP1/UAF1 complex promotes HR, at least in part by suppressing NHEJ.

The integrity of the mammalian genome is essential for the suppression of oncogenesis, and it is maintained by several intricate DNA repair mechanisms. Mammalian cells have at least six major DNA repair pathways, including mismatch repair (MMR), base excision repair (BER), nucleotide excision repair (NER), homologous recombination (HR) repair, non-homologous end joining (NHEJ), and translesion DNA synthesis (TLS) (24, 31). In general, these pathways cope with different types of DNA damage, and they exhibit differential cell cycle and tissue specificities. The mechanisms by which a cell (i) chooses among these pathways and (ii) coordinates the activities of its DNA repair pathways are largely unknown. Recent studies indicate that ubiquitin and SUMO modifications are essential to DNA repair regulation (3, 16).

The deubiquitinating enzyme (DUB) USP1 is required for the deubiquitination of FANCD2-Ub (34) and PCNA-Ub (19) and is therefore a regulator of interstrand cross-link (ICL) repair and TLS, respectively. Knockdown of USP1 results in elevated levels of FANCD2-Ub and PCNA-Ub and in increased cellular sensitivity to interstrand cross-linking agents, such as mitomycin C (MMC). Knockout of USP1 in chicken DT40 cells (36) or in a mouse model (25) results in an increase in cross-linker sensitivity and in chromosome radial formation, the hallmark of the Fanconi anemia (FA) phenotype.

USP1 binds constitutively to an 80-kDa binding partner,

referred to as UAF1 (USP1-associated factor 1). UAF1 has an N-terminal WD40 domain, with eight WD propeller sequences, and a C-terminal coiled-coil domain of unknown function. Interestingly, the WD40 domain of UAF1 binds and stimulates the ubiquitin protease activity of USP1 (10). UAF1 has also been shown to bind the DUB enzymes USP12 and USP46 (9, 40), although the substrates of the USP12/UAF1 and USP46/UAF1 complexes were previously unknown. Recent studies indicated that H2A-Ub and H2B-Ub may be substrates of these DUB complexes (23). The molecular mechanism of the USP1/UAF1 complex in DNA repair remains unknown.

In the current study, we disrupted UAF1 in the chicken B cell line DT40 (6). UAF1-deficient DT40 cells exhibited increased sensitivity to camptothecin, poly(ADP-ribose) polymerase (PARP) inhibitor, and MMC. This phenotype was epistatic with USP1 disruption. UAF1-deficient cells were defective in gene conversion and in homologous recombination. These defects were rescued by additional disruption of the Ku70 gene, a key regulator of NHEJ, in UAF1-deficient cells. We conclude that the USP1/UAF1 complex is a critical regulator of ICL repair and homologous recombination. Moreover, the USP1/UAF1 complex, together with the FA pathway, has a novel role in suppressing NHEJ.

MATERIALS AND METHODS

Cell culture. DT40 cells were cultured in RPMI 1640 medium supplemented with 10⁻⁵ M beta-mercaptoethanol, 10% fetal bovine serum (FBS), and 1% chicken serum at 39.5°C.

Generation of *USP1*^{-/-}, *UAF1*^{-/-}, and *USP1*^{-/-} *UAF1*^{-/-} double-knockout DT40 cells. Two USP1 disruption constructs, USP1-bsr and USP1-puro, were generated from genomic PCR products combined with Bsr^r and Puro^r selection marker cassettes flanked by *loxP* sites. Genomic DNA sequences were amplified

* Corresponding author. Mailing address: Department of Radiation Oncology, Dana-Farber Cancer Institute, Harvard Medical School, 44 Binney Street, Boston, MA 02115. Phone: (617) 632-2112. Fax: (617) 632-5757. E-mail: alan_dandrea@dfci.harvard.edu.

† Supplemental material for this article may be found at <http://mc.manuscriptcentral.com/mcb>.

∇ Published ahead of print on 11 April 2011.

using the primers 5'-AAATGGGCAATTTACAGTTTGCATCGG-3' and 5'-TGCTAATTGTAATGCCACTGTGCATCAC-3' (for the left arm of the targeting construct and the probe for Southern blotting) and 5'-TCGTCATCTACATCAACTCCTTACCTAC-3' and 5'-AACTACGGCTCTGTTTCAAAGACTTCAC-3' (for the right arm of the targeting construct). Each amplified 3.2-kb PCR product, including the left arm, and 5.0-kb PCR product, including the right arm, was cloned into the pCR2.1-TOPO vector (Invitrogen, CA). The vector with the 3.2-kb PCR product was digested with HindIII to remove the 1.3 kb of template sequence for amplifying the Southern blotting probe. The remaining product, including 1.9 kb of the left arm, was self-ligated at the HindIII sites and then digested with NotI and XhoI. The vector cloned with the 5.0-kb PCR product was digested with NotI and XhoI, and 3.9 kb of right arm was extracted. Then, the 3.9-kb right arm was cloned into NotI and XhoI sites of the vector carrying the 1.9-kb left arm. The Bsr^r and Puro^r selection marker genes flanked by *loxP* sequences were blunted and inserted into the blunted NotI site of the vector carrying the left and right arms to generate the USP1-bsr and USP1-puro disruption constructs. The 0.5-kb fragment generated by PCR from 1.3 kb of template sequence using the primers 5'-AAATGGGCAATTTACAGTTTGCATCGG-3' and 5'-CAGAGGAAGTTCCTGTCTACTTTGTC-3' was used as a probe for Southern blot analysis. To generate *USP1*^{-/-} cells, linearized USP1 disruption constructs were transfected sequentially by electroporation (Bio-Rad). The genomic DNA of the transfectants was digested with BamHI, and the targeted clones were confirmed by Southern blot analysis.

Three UAF1 disruption constructs, UAF1-puro, UAF1-his, and UAF1-hyg, were also generated from genomic PCR products combined with Puro^r, His^r, and Hyg^r selection cassettes flanked by *loxP* sites using the MultiSite Gateway technology (Invitrogen, Carlsbad, CA). All procedures were performed according to the manufacturer's instructions. Genomic DNA sequences were amplified using the primers 5'-GGGGACAACCTTTGTATAGAAAAGTTGACCTCTATTAGCTCCAC-3' and 5'-GGGGACTGCTTTTTTGTACAAAAGTTGGCAAATCC TTTATGCGC-3' (for the left arm of the targeting construct) and 5'-GGGGA CAGCTTCTGTACAAAAGTTGAGCCACATATCGAGTCCA-3' and 5'-G GGGACAACCTTTGTATAATAAAGTTGCCAGCATCTTTTGTCTGAA-3' (for the right arm of the targeting construct). To generate the left and the right arm entry clones, each 1.4 kb of the left arm and 3.5 kb of the right arm was subcloned into the donor vector pDONRP4-P1R and pDONRP2R-P3, respectively, by BP recombination. To generate the targeting vector by LR recombination, we used the left and the right arm entry clones, pDEST DTA-MLS, and Puro/His/Hyg entry clone (20). The 0.4-kb fragment generated by PCR of genomic DNA using the primers 5'-ACCGAAATGGGGTAAATGCACTTCA GC-3' and 5'-GAGTTCACAAAAGGTCATTCG-3' was used as a probe for Southern blot analysis. To generate *UAF1*^{-/-} cells, linearized UAF1 disruption constructs were transfected sequentially by electroporation (Bio-Rad). The genomic DNA of the transfectants was digested with NotI and EcoRI, and the targeted clones were confirmed by Southern blot analysis. To establish cell lines that stably expressed the human UAF1 transgene (*UAF1*^{-/-}; *hUAF1* cells), the pcDNA3.1-hUAF1 (10) expression vector was used.

To generate *USP1*^{-/-} *UAF1*^{-/-} cells, selection cassettes were excised from the *UAF1*^{-/-} lines by the transient transfection of Cre recombinase expression vector and addition of 50 nM 5-hydroxytamoxifen to the medium for Cre recombinase induction. Depletion of the selection cassettes in *UAF1*^{-/-} cells was confirmed by the restored sensitivity to all selection drugs. Subsequently, targeting constructs of USP1 were transfected, and disruption of USP1 was confirmed by Southern analysis and reverse transcription-PCR (RT-PCR).

Generation of *UAF1*^{-/-} *Ku70*^{-/-} double-knockout DT40 cells. To generate the *UAF1*^{-/-} *Ku70*^{-/-} cells, targeting constructs of Ku70 (Ku70-his and Ku70-hyg) described previously (42) were transfected sequentially in *UAF1*^{-/-} cells from which selection cassettes were depleted. The disruption of Ku70 was confirmed by Southern analysis.

Antibodies and immunoblotting. The following antibodies were used: anti-UAF1 (rabbit polyclonal) (10); anti-chicken FANCD2 (rabbit polyclonal) (21); anti-USP1 (A301-699A; Bethyl Laboratories, Montgomery, TX); anti-PCNA (mouse monoclonal, sc-56; Santa Cruz Biotechnology); anti-lamin B1 (rabbit polyclonal, ab16048; Abcam), and antiactin (mouse monoclonal; Sigma, St. Louis, MO).

Measurement of cellular sensitivity to DNA-damaging agents. A methylcellulose colony formation assay was performed as described previously (42). Briefly, to assess ionizing radiation (IR) sensitivity, serially diluted cells were plated in medium containing 1.5% (wt/vol) methylcellulose, incubated for 1 h at 39.5°C, and irradiated with a ¹³⁷Cs source. To measure the sensitivity of cells to camptothecin, cells were continuously exposed to various concentrations of camptothecin mixed in medium containing methylcellulose to allow the cells to pass through multiple rounds of DNA replication. For exposure of cell to UV, 3 × 10⁵

cells were suspended in 0.5 ml of phosphate-buffered saline (PBS) containing 1% FBS in the six-well plates and irradiated with UV-C (wavelength, 254 nm). For exposure of cells to MMC, 3 × 10⁵ cells were treated at 39.5°C in 1 ml of complete medium containing MMC for 1 h. As for treatment with the PARP inhibitor (Olaparib; AZD2281; Selleck Chemicals, TX), 3,000 cells were seeded into 24-well plates in 1 ml culture medium per well, exposed to various concentrations of PARP inhibitor, and then incubated at 39.5°C for 72 h. To assess the number of live cells, we measured the amount of ATP by using a CellTiter-Glo luminescence cell viability assay kit (Promega Corporation, Madison, WI).

I-SceI-induced gene conversion of SCneo. Modified SCneo (15) was inserted into the previously described *Ovalbumin* gene construct and then targeted into the *Ovalbumin* locus in wild type, *UAF1*^{-/-}, *USP1*^{-/-}, *USP1*^{-/-} *UAF*^{-/-}, *Ku70*^{-/-}, and *UAF1*^{-/-} *Ku70*^{-/-} cells. In the transient-transfection assays, 5 × 10⁶ cells were suspended in 500 μl of PBS mixed with each of several circular plasmid DNAs (30 μg; empty vector [pcDNA3.1], wild type human UAF1, WD40 repeat 2 deleted human UAF1 [10], and I-SceI expression vector [pCB-ASce]), and electroporated using the Bio-Rad electroporation system (250 V, 960 μF). Cells were incubated for 24 h, serially diluted, and plated onto methylcellulose containing 2 mg/ml neomycin; a control set was plated into methylcellulose without neomycin. After 7 to 10 days, colonies appeared and were counted. We evaluated the gene conversion rate as the percent ratio of colonies growing in neomycin versus colonies growing in the control dish without neomycin.

Flow cytometric analysis of cell cycle progression. Cells were harvested, fixed with 70% ethanol, and resuspended in PBS containing propidium iodide (PI) at 5 μg/ml for subsequent analysis with a FACScalibur apparatus. The data were processed using Cell Quest (Becton Dickinson).

Immunofluorescence. Cells were incubated with camptothecin at 100 nM for 1 h and then washed with PBS 3 times and cultured in normal RPMI medium. Cells were harvested at 0, 1, and 6 h after exposure to the drug and spun down by using a cytospin centrifuge (Thermo Scientific). The slides were fixed with 4% paraformaldehyde in PBS for 10 min, permeabilized with 0.1% NP-40 in PBS buffer for 20 min, and blocked with 3% bovine serum albumin in PBS with 0.05% Tween 20 (PBST) at room temperature. Fixed slides were costained with anti-pH2AX (1:1,000; Millipore) and anti-Rad51 (1:100; Santa Cruz Biotechnology). Next, slides were washed with PBST and incubated with secondary antibodies (1:2,000; Invitrogen) for 1 h. Slides were stained and mounted with 4',6-diamidino-2-phenylindole-containing mounting medium (Vector Laboratories).

RESULTS

Generation of *USP1*^{-/-}, *UAF1*^{-/-}, and *USP1*^{-/-} *UAF1*^{-/-} double-knockout DT40 cells. To elucidate the function of USP1 and UAF1 in DNA repair and to examine the epistatic relationship between USP1 and UAF1, we generated *USP1*^{-/-}, *UAF1*^{-/-}, and *USP1*^{-/-} *UAF1*^{-/-} chicken DT40 cells. In accordance with a previous report (36), we designed a targeting construct to delete the last exon of USP1, encoding a histidine motif that is essential for catalytic activity (34) (see Fig. S2A in the supplemental material). We confirmed the serial disruption of the USP1 gene by Southern analysis and Western blotting (see Fig. S2B and D). The amino acid sequence identity between human UAF1 and chicken UAF1 is 98% (see Fig. S1). UAF1 is composed of eight WD40 motifs that are essential for binding USP1. Deletion of the WD40 repeat 2 of UAF1 disrupts its propeller-like structure and disrupts USP1 binding (10). Therefore, we designed targeting constructs with WD40 repeats 2 through 5 deleted (Fig. 1A). The chicken UAF1 gene lies on chromosome 2 and is trisomic in DT40 cells (39). Thus, three disruption constructs (UAF1-puro, UAF1-his, and UAF1-hyg), with selection cassettes flanked by *loxP* sites, were sequentially transfected into DT40 cells, in order to generate a *UAF1*^{-/-} clone. Southern analysis demonstrated the sequential disruption of the UAF1 gene (Fig. 1B). We confirmed the disruption of *UAF1* in *UAF1*^{-/-} cells by Western blotting (Fig. 1D, upper gel).

To generate double-knockout cells of USP1 and UAF1, se-

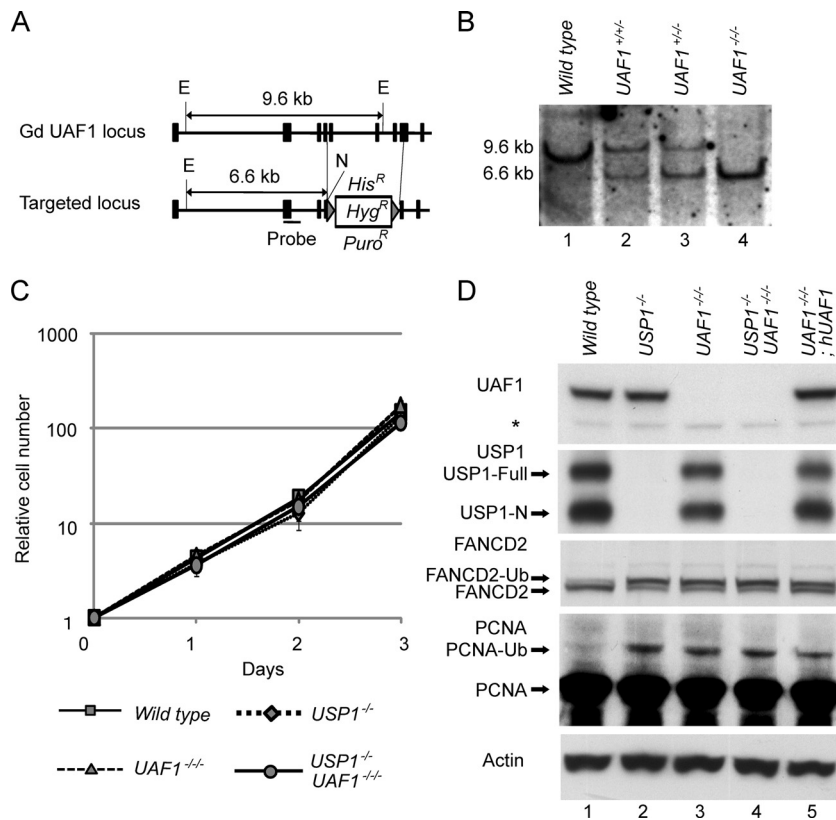


FIG. 1. Targeted disruption of chicken UAF1 and characterization of DT40 mutants. (A) Schematic representation of the chicken UAF1 locus and configuration of the targeted allele. E, EcoRI; N, NotI. The fourth to the eighth exons, which includes the WD40 domain, were deleted by gene disruption. Solid squares indicate the positions of exons. The probe used in the Southern blot analysis is indicated as a horizontal bar. Each resistance gene is flanked by *loxP* sites (gray triangles). (B) Southern blot analysis of EcoRI- and NotI-digested genomic DNA from cells with the indicated genotypes, using the flanking probe shown in panel A. (C) Growth curves of cells of the indicated genotypes. The error bars represent standard deviations ($n = 3$). (D) Western blot analysis of whole-cell lysates prepared from the indicated genotypes. Cells were probed with anti-UAF1, anti-USP1, anti-chicken FANCD2, anti-PCNA, and antiactin antibodies. The asterisk indicates a nonspecific band.

lection cassettes were excised from the *UAF1*^{-/-} cells by transient overexpression of Cre recombinase. The USP1 gene was thereby depleted in the *UAF1*^{-/-} clone. The disruption of USP1 in *UAF1*^{-/-} cells was confirmed by Southern blotting (see Fig. S2B in the supplemental material), RT-PCR (data not shown), and Western blotting (see Fig. S2C and D). The proliferative properties of mutant cells were indistinguishable from those of wild-type cells, as monitored by growth curves (Fig. 1C) and by cell cycle analysis (data not shown).

Epistatic relationship of USP1 and UAF1 in deubiquitination of FANCD2 and PCNA. Previous studies demonstrated that the disruption of USP1 or UAF1 results in an increase in the endogenous monoubiquitination levels of both PCNA and FANCD2. To confirm the functional disruption of USP1 and UAF1, we performed Western blot assays using anti-chicken FANCD2 antibody (21) and anti-PCNA antibody. The monoubiquitination levels of both FANCD2 and PCNA were elevated in *USP1*^{-/-} and *UAF1*^{-/-} cells, even in the absence of exogenous DNA damage (Fig. 1D, lanes 2 and 3). The monoubiquitination level of FANCD2 and PCNA did not exhibit any further increase in the *USP1*^{-/-} *UAF1*^{-/-} cells, suggesting that USP1 and UAF1 are epistatic for the deubiquitination of FANCD2 and PCNA (Fig. 1D, lane 4).

In an attempt to complement the *UAF1*^{-/-} cells, we over-

expressed Flag-tagged human UAF1 cDNA in *UAF1*^{-/-} cells (here referred to as *UAF1*^{-/-}; *hUAF1* cells) (10) by random integration. *UAF1*^{-/-}; *hUAF1* cells exhibited partial reduction of the high monoubiquitination levels of FANCD2 and PCNA observed in *UAF1*^{-/-} cells (Fig. 1D, lane 5).

Epistatic relationship of USP1 and UAF1 in cellular sensitivity to DNA-damaging agents. To assess the functions of USP1 and UAF1 and their epistatic relationship in DNA repair, we examined the cellular sensitivity to various DNA-damaging agents. Consistent with previous reports (25, 36), USP1 ablation resulted in hypersensitivity to the cross-linking agent MMC and marginally increased sensitivity to UV (Fig. 2D and E). There was no increase in the sensitivity to IR (Fig. 2A). Interestingly, *USP1*^{-/-} cells were hypersensitive to camptothecin and PARP inhibitor, compared to wild-type cells (Fig. 2B and C). *UAF1*^{-/-} cells showed similar sensitivity to *USP1*^{-/-} cells with respect to all DNA-damaging agents tested. Exogenous expression of human UAF1 rescued the hypersensitivity of *UAF1*^{-/-} to MMC, and UV completely and partially restored the sensitivity to camptothecin and PARP inhibitor. USP1 disruption in *UAF1*^{-/-} cells had no additive impact on the sensitivity to DNA-damaging agents, confirming that USP1 and UAF1 are epistatic in a common DNA repair pathway.

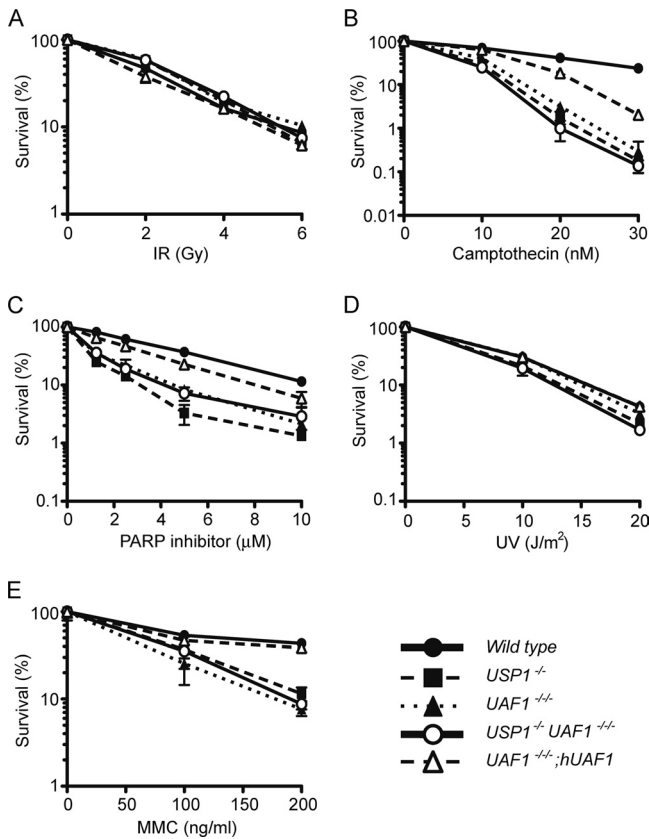


FIG. 2. Epistatic analysis of *UAF1*^{-/-}, *USP1*^{-/-}, and *USP1*^{-/-} *UAF1*^{-/-} cells. Sensitivity curve show results for cells to various DNA-damaging agents in wild-type and the indicated mutant cells. (A, B, D, and E) The fraction of surviving colonies in methylcellulose plates for each agent. (C) PARP inhibitor sensitivity, determined by cell viability (based on the ATP level) of mutant cells. The error bars represent standard deviations (*n* = 3).

UAF1 promotes homology-directed I-SceI-induced DSB repair. It is known that camptothecin blocks topoisomerase I in a state where it is covalently linked to nicked DNA. The resulting protein/DNA cross-links obstruct DNA replication and transcription, and these lesions are repaired by single-strand break (SSB) repair. If a replication fork moves through a nick, it creates a double-strand break (DSB) that must be repaired by HR. Hence, HR-deficient cells are well known to be hypersensitive to camptothecin (1).

Furthermore, HR-deficient cells, such as BRCA1, BRCA2/FANCD1, or FA pathway-deficient cells, are hypersensitive to PARP inhibitor (29, 30), since PARP inhibition leads to failure of SSB repair, resulting in the formation of DSBs during replication. Therefore, the hypersensitivity to camptothecin and PARP inhibitor suggests an impairment in HR in *USP1*^{-/-} cells and *UAF1*^{-/-} cells. To investigate the involvement of UAF1 in HR-mediated repair directly, we measured gene conversion induced by the rare-cutting endonuclease I-SceI, using the *SCneo* substrate (17). Specifically, we integrated the *SCneo* substrate into the *Ovalbumin* locus (15) and measured the efficiency of I-SceI-induced gene conversion in various DT40 mutants. While 2.5% of the wild-type cells successfully underwent gene conversion and reconstituted neomycin resistance,

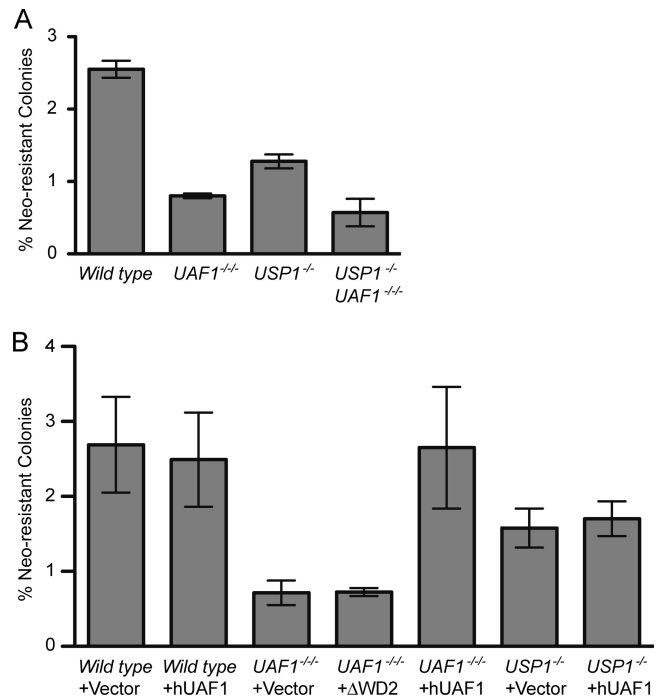


FIG. 3. *UAF1*-deficient cells have a severe defect in HR repair. (A and B) Cells with the indicated genotypes, containing the integrated *SCneo* substrate, were transiently transfected with the I-SceI endonuclease expression vector and plated in methylcellulose-containing medium with or without neomycin selection. The gene conversion frequency was calculated as the percentage of neomycin-resistant colonies relative to the number of colonies plated in neomycin-free methylcellulose. +Vector, +hUAF1, or +hUAF1-ΔWD2 indicate transient expression of I-SceI, together with pcDNA3.1 empty vector, wild-type human UAF1, or WD40 repeat 2-deleted human UAF1.

the same reaction occurred in only 0.80%, 1.28%, and 0.57% of the *UAF1*^{-/-}, *USP1*^{-/-}, and *USP1*^{-/-} *UAF1*^{-/-} cells, respectively. These results again showed the epistatic effect of the *USP1* and *UAF1* genes (Fig. 3A). The more severe defect for HR in the *UAF1*-deficient cells, compared to the *USP1*^{-/-} cells, suggests that *UAF1* may bind and stimulate other USPs that contribute to HR repair in the absence of *USP1*. Previous studies indicated that *UAF1* binds and stimulates multiple DUBs, including *USP1*, *USP12*, and *USP46* (9, 40). Our results suggest that in the *USP1*^{-/-} cells, *USP12/UAF1* and/or *USP46/UAF1* complexes may also contribute to HR activity.

Expression of wild-type human *UAF1* in *UAF1*^{-/-} cells rescued the rate of gene conversion to wild-type levels, although a mutant form of human *UAF1*-ΔWD2 which lacks the WD40 repeat 2 and which was previously described (10) failed to rescue the gene conversion in the *UAF1*^{-/-} cells. On the other hand, expression of wild-type human *UAF1* in wild-type and *USP1*^{-/-} cells did not affect their gene conversion rates (Fig. 3B). These results together indicate that both *UAF1* and *USP1* are required for normal HR repair.

FANCD2 is monoubiquitinated following camptothecin exposure. To determine if the FA pathway is active in the repair of camptothecin-induced lesions, we examined the kinetics of monoubiquitination of FANCD2 at several time points following camptothecin (30 nM) exposure. For wild-type cells, the

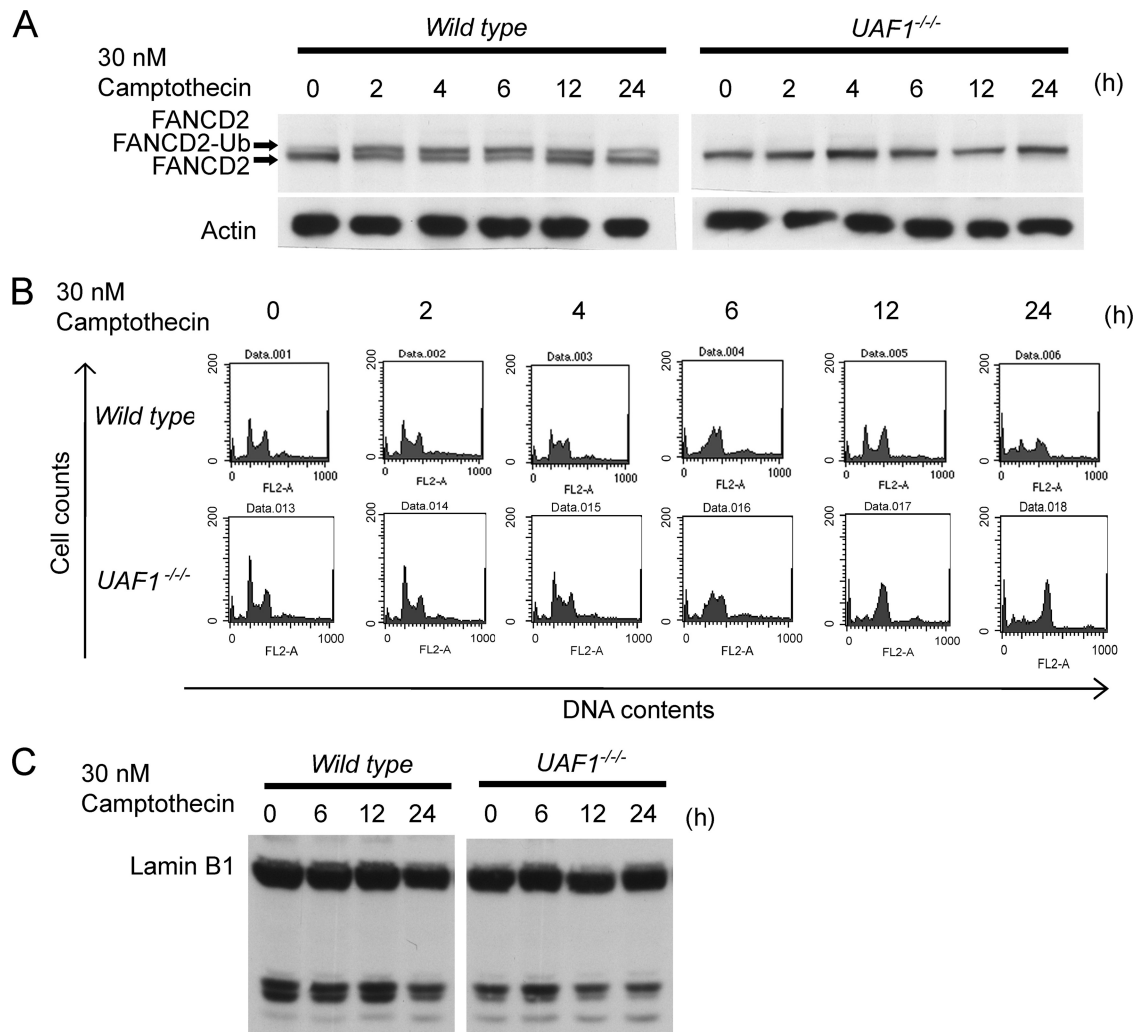


FIG. 4. Camptothecin induces accumulation in the 4N population in *UAF1*^{-/-} cells. (A) Western blot analysis of whole-cell lysates prepared from wild-type and *UAF1*^{-/-} cells probed with the indicated antibodies. Cells were treated with camptothecin (30 nM) continuously and lysed 2, 4, 6, 12, or 24 h later. (B) Cell cycle profiles. Cells were treated with 30 nM camptothecin for 2, 4, 6, 12, or 24 h and analyzed by flow cytometry. (Top) Wild-type cells; (bottom) *UAF1*^{-/-} cells. (C) Western blot analysis of whole-cell lysates prepared from cells of the indicated genotypes and probed with anti-lamin B1 after treatment with camptothecin (30 nM) continuously and then lysed 6, 12, or 24 h later.

monoubiquitination level of FANCD2 was increased after 2 h and remained elevated 6 h after camptothecin exposure (Fig. 4A, left panel). The level was decreased 12 h after camptothecin treatment, consistent with the recovery of the cell cycle at this time (Fig. 4B, upper graphs). In contrast, the monoubiquitination of FANCD2 persisted in the *UAF1*^{-/-} cells at all time points (Fig. 4A, right panel), and G₂/M accumulation in the 4N population remained elevated as well (Fig. 4B, lower graphs). No degradation of lamin B1 protein was observed in the same time frame (Fig. 4C), suggesting that the *UAF1*^{-/-} cells die from impaired repair of camptothecin-induced lesions and not from camptothecin-induced apoptosis. These results raise the possibility that ubiquitination and deubiquitination of FANCD2 by the USP1/UAF1 complex is involved in the repair of camptothecin-induced lesions.

We also generated heterozygous mutant knockout clones of DT40, for either the *UAF1* or *USP1* locus (see Fig. S3 in the supplemental material). A gene dosage effect was not observed

for the deubiquitination of FANCD2-Ub or PCNA-Ub in the absence of DNA damage (see Fig. S3A). However, a slight decrease in the rate of deubiquitination following camptothecin exposure was observed for the *UAF1*^{+/-} genotype compared to the *UAF1*^{+/+} clone (see Fig. S3B).

UAF1 promotes HR by suppressing NHEJ. In eukaryotic cells, DSBs are predominantly repaired either through HR (error-free repair) or NHEJ (error-prone repair). HR-deficient cells, but not NHEJ-deficient cells, such as *Ku70* or DNA ligase IV-deficient cells, are hypersensitive to camptothecin (11). Moreover, *Ku70*^{-/-} DT40 cells tend to be more resistant to camptothecin than wild-type cells, suggesting that NHEJ may normally suppress HR (1). Therefore, the NHEJ pathway appears to have two effects, one to promote survival by end joining of DSBs and the other to reduce survival by inaccurate end joining or toxic effects after DSBs. To better appreciate the importance of *UAF1* in HR, we disrupted *Ku70* in *UAF1*^{-/-} cells. Because HR is the only DNA repair pathway available for

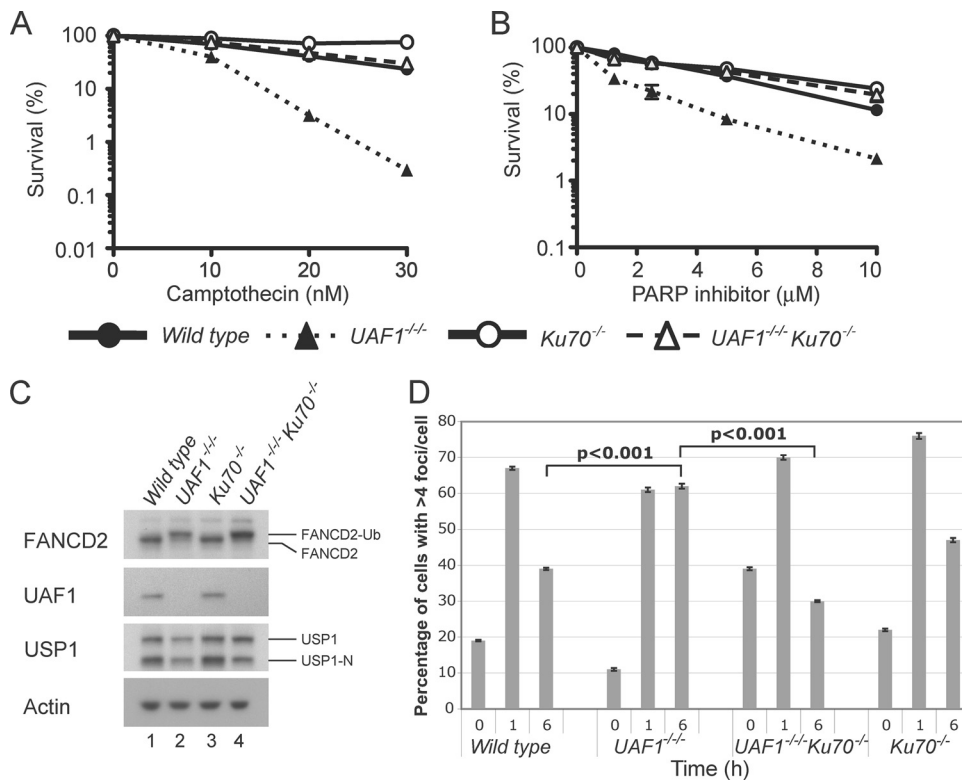


FIG. 5. Restoration of camptothecin and PARP inhibitor resistance by disruption of NHEJ in *UAF1*-deficient cells. (A and B) Sensitivity curves of cells to DNA-damaging agents in the indicated mutants. (A) The fraction of colonies surviving camptothecin in methylcellulose plates. The error bars represent standard deviations ($n = 3$). (B) PARP inhibitor sensitivity, determined by cell viability (based on ATP levels) of mutant cells. The error bars represent standard deviations ($n = 3$). (C) Western blotting of the cell lines used in panels A and Bs, using the indicated antibody. (D) Time course of Rad51 foci formation after 100 nM camptothecin-induced DNA damage for 1 h. Cells with five or more Rad51 foci per cell were scored as positive.

dealing with DSBs in *Ku70*^{-/-} cells, the difference would determine the involvement of UAF1 in HR-mediated DSB repair.

There were no significant differences in the cell cycle distributions among wild-type, *UAF1*^{-/-}, *Ku70*^{-/-}, and *UAF1*^{-/-} *Ku70*^{-/-} cells (data not shown). Interestingly, the resistance to camptothecin was restored in *UAF1*^{-/-} *Ku70*^{-/-} cells compared to single *UAF1*^{-/-} cells (Fig. 5A), suggesting that the toxic effects of NHEJ were dominant in *UAF1*^{-/-} cells. UAF1 appears to counteract Ku70 or NHEJ function in the repair of camptothecin-induced lesions, preventing cells from entering the NHEJ repair pathway. By the same token, the sensitivity to PARP inhibitor was also restored in *UAF1*^{-/-} *Ku70*^{-/-} cells compared to single *UAF1*^{-/-} cells (Fig. 5B).

We next examined the activity of the FA pathway in the various DT40 clones (Fig. 5C). As expected, the disruption of UAF1 resulted in an upregulation of FANCD2 monoubiquitination, and FANCD2-Ub levels were unaffected by Ku70 disruption (lanes 3 and 4). USP1 levels were slightly lower in the *UAF1*-deficient clones (lanes 2 and 4), consistent with previous reports indicating that UAF1 stabilizes USP1 (10).

The rescue of camptothecin resistance in the *UAF1*^{-/-} *Ku70*^{-/-} double-knockout cells suggested that these cells have restored HR repair. To further test this hypothesis, we measured the kinetics of Rad51 foci assembly in the various sub-

clones (Fig. 5D). Camptothecin stimulated Rad51 foci in wild-type cells at 1 h, with a rapid decline in Rad51 foci by 6 h post-camptothecin exposure. *UAF1*^{-/-} cells displayed a defect in HR repair, demonstrated by the persistence of Rad51 foci in 60% of the cells, even 6 h after camptothecin (Fig. 5D; see also Fig. S4 in the supplemental material). Interestingly, in the *UAF1*^{-/-} *Ku70*^{-/-} cells, Rad51 foci resolved more quickly, consistent with the measured improvement in HR repair. Taken together, these results suggest that UAF1 functions, at least in part, to promote the rapid assembly and disassembly of Rad51 foci and that Ku70 reduces the rate of Rad51 foci. Knockout of Ku70 restores the rapid disassembly of the Rad51 foci.

The I-SceI-induced gene conversion assay demonstrated that the transient overexpression of human UAF1 in *UAF1*^{-/-} *Ku70*^{-/-} cells slightly increased the HR efficiency compared to the parental *UAF1*^{-/-} *Ku70*^{-/-} cells (Fig. 6). Taken together, our results demonstrate that UAF1 promotes DSB-induced HR.

DISCUSSION

Increasing evidence indicates that protein ubiquitination is an important regulatory mechanism for DNA repair pathways (18). Protein ubiquitination is regulated by the coordinate activity of E3 ubiquitin ligases and DUBs. While there are more

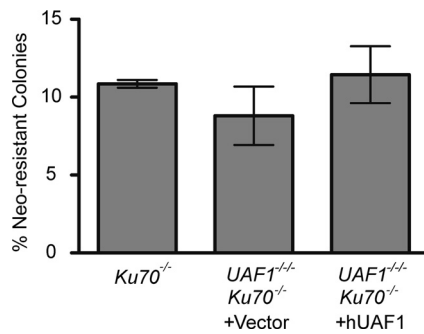


FIG. 6. UAF1 promotes HR-mediated DSB repair. Cells with the indicated genotypes, carrying an integrated SCneo substrate, were treated as described for Fig. 3. +Vector and +hUAF1 indicate transient expression of I-SceI together with pcDNA3.1 empty vector and wild-type human UAF1, respectively. The error bars represent standard deviations ($n = 3$).

than 500 E3 ligases encoded by the human genome, only 100 DUB enzymes are known (35).

The mechanisms by which protein ubiquitination regulates DNA repair are largely unknown. On the one hand, protein monoubiquitination results in the recruitment of key effector proteins with monoubiquitin binding domains, such as UBZ or UBM domains (4). For instance, PCNA monoubiquitination recruits UBZ-containing TLS polymerases to DNA at the site of DNA lesion bypass (4). Also, FANCD2 monoubiquitination recruits the UBZ-containing FAN1 nuclease to sites of DNA cross-link repair (26–28, 38). On the other hand, protein polyubiquitination has recently been shown to promote DNA repair protein recruitment to sites of damaged chromatin (12, 41).

The mechanisms by which DUB enzymes regulate DNA repair are also largely unknown. Multiple DUBs have been implicated in DNA repair or cell cycle checkpoint regulation, including USP1 (34), USP3 (33), USP11 (43), and USP28 (44). USP1 regulates DNA repair by controlling the monoubiquitination state of its two substrates, FANCD2-Ub (34) and PCNA-Ub (19), and USP1 is bound and activated by the UAF1 protein (10). Studies to date indicate that efficient DNA repair requires both the monoubiquitination of these substrates, by the FA core complex or the RAD18 enzyme, respectively, and their coordinated deubiquitination. Disruption of either ubiquitination or deubiquitination results in an abnormality in DNA repair.

In the current study, we examined the role of the DUB complex, USP1/UAF1, in DNA repair. Disruption of USP1 and/or UAF1 in DT40 cells resulted in elevated FANCD2-Ub and PCNA-Ub levels. Interestingly, USP1 and UAF1 were epistatic in an HR pathway, and knockout of each gene, alone or in combination, resulted in a comparable level of substrate monoubiquitination and camptothecin sensitivity. Moreover, we provided evidence that the USP1/UAF1 complex regulates DNA repair by promoting HR repair. Disruption of USP1 and/or UAF1 results in reduced HR, as judged by the reduced values in the SCneo assay.

However, how UAF1 expression promotes HR activity is not known. One possibility is that the USP1/UAF1 complex can release the monoubiquitinated FANCD2/FANCI complex from chromatin, deubiquitinate FANCD2 and FANCI, and recycle these proteins for additional DNA repair events. Dis-

ruption of UAF1 or USP1 may result in depleted pools of free FANCD2 and FANCI or in the accumulation of monoubiquitinated FANCD2/FANCI complex, which may interfere with normal replication fork progression or DNA repair.

Other recent studies suggest a role of protein ubiquitination in the regulation of HR repair. For instance, the ubiquitin conjugating enzyme, UBC13, initiates HR activity (45). Also, proteasome inhibition can disrupt HR function (22, 32). The relative role of ubiquitin E3 ligases and DUBs in regulating HR is an important emerging field in DNA repair research.

Other recent studies suggested the presence of regulatory mechanisms in the cell which suppress NHEJ and thereby promote HR repair. For instance, the FA pathway suppresses NHEJ and promotes HR. Disruption of the NHEJ protein Ku70 rescues HR in FANCC-deficient cells (37), and disruption of the NHEJ protein DNA-PK promotes HR in FANCD2-deficient cells (2). Still other studies have indicated that the DNA repair regulatory protein, BRCA1, can also suppress NHEJ (5, 7, 8). BRCA1 appears to displace the NHEJ pathway-related protein 53BP1 from the site of double-strand breaks. Loss of BRCA1 leads to increased 53BP1-mediated NHEJ activity and to increased toxicity due to chromosome breakage and translocations. A secondary loss in 53BP1 results in a rescue of these cells, a decrease in NHEJ, and a compensatory increase in HR. It will be important to determine the mechanism by which the USP1/UAF1 complex suppresses NHEJ and promotes HR and whether this is the same mechanism as with the FA pathway. The mechanism of NHEJ suppression is largely unknown. According to one model, USP1/UAF1 may suppress NHEJ and promote HR by enhancing the processing of DSBs into forms with free (exposed) 3' ends which are more suitable for strand invasion of the homologous template.

We propose a model in which the FA pathway can function to suppress Ku70-driven NHEJ and to promote HR repair. For cells in which USP1 or UAF1 is lost, there is no longer suppression of NHEJ-driven DSB repair. In this case, elevated Ku70-driven NHEJ leads to toxicity and camptothecin-driven cell death. However, if there is an additional loss of Ku70, as in *UAF1*^{-/-} *Ku70*^{-/-} double knockout DT40 cells, there is a loss of toxic NHEJ and a rescue of HR repair. Hence, the double-knockout cells have improved survival in the presence of camptothecin and PARP inhibitor. Consistent with this model, the *UAF1*^{-/-} *Ku70*^{-/-} double-knockout cells exhibit persistently elevated FANCD2-Ub levels (Fig. 5B) but have restored camptothecin-induced Rad51 foci assembly and disassembly (Fig. 5C). It will be interesting to determine whether these double-knockout cells retain some defect resulting from their elevated FANCD2-Ub or PCNA-Ub levels.

In summary, our results demonstrate that the USP1/UAF1 complex plays a critical role as a positive regulator for HR repair. Accordingly, disruption of USP1/UAF1 may provide a potent method for blocking HR repair and sensitizing cells to DNA interstrand cross-linking agents, or to the new class of PARP inhibitors which have entered clinical trials (13, 14).

ACKNOWLEDGMENTS

We thank Minoru Takata for the anti-chicken FANCD2 antibody. We also thank members of the D'Andrea laboratory for helpful discussions.

J.M. was funded by long-term research grants from the TOYOBO Biotechnology Foundation. K.Y. is a Harvard University Presidential Scholar. This work was supported by NIH grants P01CA092584, R01DK43889, and R01HL52725 to A.D.D.

REFERENCES

- Adachi, N., S. So, and H. Koyama. 2004. Loss of nonhomologous end joining confers camptothecin resistance in DT40 cells. Implications for the repair of topoisomerase I-mediated DNA damage. *J. Biol. Chem.* **279**:37343–37348.
- Adamo, A., et al. 2010. Preventing nonhomologous end joining suppresses DNA repair defects of Fanconi anemia. *Mol. Cell* **39**:25–35.
- Bergink, S., and S. Jentsch. 2009. Principles of ubiquitin and SUMO modifications in DNA repair. *Nature* **458**:461–467.
- Bienko, M., et al. 2005. Ubiquitin-binding domains in Y-family polymerases regulate translesion synthesis. *Science* **310**:1821–1824.
- Bouwman, P., et al. 2010. 53BP1 loss rescues BRCA1 deficiency and is associated with triple-negative and BRCA-mutated breast cancers. *Nat. Struct. Mol. Biol.* **17**:688–695.
- Buerstedde, J. M., and S. Takeda. 1991. Increased ratio of targeted to random integration after transfection of chicken B cell lines. *Cell* **67**:179–188.
- Bunting, S. F., et al. 2010. 53BP1 inhibits homologous recombination in Brca1-deficient cells by blocking resection of DNA breaks. *Cell* **141**:243–254.
- Cao, L., et al. 2009. A selective requirement for 53BP1 in the biological response to genomic instability induced by Brca1 deficiency. *Mol. Cell* **35**:534–541.
- Cohn, M. A., Y. Kee, W. Haas, S. P. Gygi, and A. D. D'Andrea. 2009. UAF1 is a subunit of multiple deubiquitinating enzyme complexes. *J. Biol. Chem.* **284**:5343–5351.
- Cohn, M. A., et al. 2007. A UAF1-containing multisubunit protein complex regulates the Fanconi anemia pathway. *Mol. Cell* **28**:786–797.
- Connelly, J. C., and D. R. Leach. 2004. Repair of DNA covalently linked to protein. *Mol. Cell* **13**:307–316.
- Doil, C., et al. 2009. RNF168 binds and amplifies ubiquitin conjugates on damaged chromosomes to allow accumulation of repair proteins. *Cell* **136**:435–446.
- Fong, P. C., et al. 2009. Inhibition of poly(ADP-ribose) polymerase in tumors from BRCA mutation carriers. *N. Engl. J. Med.* **361**:123–134.
- Fong, P. C., et al. 2010. Poly(ADP)-ribose polymerase inhibition: frequent durable responses in BRCA carrier ovarian cancer correlating with platinum-free interval. *J. Clin. Oncol.* **28**:2512–2519.
- Fukushima, T., et al. 2001. Genetic analysis of the DNA-dependent protein kinase reveals an inhibitory role of Ku in late S-G2 phase DNA double-strand break repair. *J. Biol. Chem.* **276**:44413–44418.
- Galanty, Y., et al. 2009. Mammalian SUMO E3-ligases PIAS1 and PIAS4 promote responses to DNA double-strand breaks. *Nature* **462**:935–939.
- Hochegger, H., et al. 2006. PARP-1 protects homologous recombination from interference by Ku and Ligase IV in vertebrate cells. *EMBO J.* **25**:1305–1314.
- Huang, T. T., and A. D. D'Andrea. 2006. Regulation of DNA repair by ubiquitylation. *Nat. Rev. Mol. Cell Biol.* **7**:323–334.
- Huang, T. T., et al. 2006. Regulation of monoubiquitinated PCNA by DUB autocleavage. *Nat. Cell Biol.* **8**:339–347.
- Iizumi, S., et al. 2006. Simple one-week method to construct gene-targeting vectors: application to production of human knockout cell lines. *Biotechniques* **41**:311–316.
- Ishiai, M., et al. 2008. FANCI phosphorylation functions as a molecular switch to turn on the Fanconi anemia pathway. *Nat. Struct. Mol. Biol.* **15**:1138–1146.
- Jacquemont, C., and T. Taniguchi. 2007. Proteasome function is required for DNA damage response and fanconi anemia pathway activation. *Cancer Res.* **67**:7395–7405.
- Joo, H. Y., et al. 2011. Regulation of histone H2A and H2B deubiquitination and Xenopus development by USP12 and USP46. *J. Biol. Chem.* **286**:7190–7201.
- Kennedy, R. D., and A. D. D'Andrea. 2006. DNA repair pathways in clinical practice: lessons from pediatric cancer susceptibility syndromes. *J. Clin. Oncol.* **24**:3799–3808.
- Kim, J. M., et al. 2009. Inactivation of murine Usp1 results in genomic instability and a Fanconi anemia phenotype. *Dev. Cell* **16**:314–320.
- Kratz, K., et al. 2010. Deficiency of FANCD2-associated nuclease KIAA1018/FAN1 sensitizes cells to interstrand crosslinking agents. *Cell* **142**:77–88.
- Liu, T., G. Ghosal, J. Yuan, J. Chen, and J. Huang. 2010. FAN1 acts with FANCI-FANCD2 to promote DNA interstrand cross-link repair. *Science* **329**:693–696.
- MacKay, C., et al. 2010. Identification of KIAA1018/FAN1, a DNA repair nuclease recruited to DNA damage by monoubiquitinated FANCD2. *Cell* **142**:65–76.
- McCabe, N., et al. 2005. BRCA2-deficient CAPAN-1 cells are extremely sensitive to the inhibition of Poly (ADP-Ribose) polymerase: an issue of potency. *Cancer Biol. Ther.* **4**:934–936.
- McCabe, N., et al. 2006. Deficiency in the repair of DNA damage by homologous recombination and sensitivity to poly(ADP-ribose) polymerase inhibition. *Cancer Res.* **66**:8109–8115.
- Moldovan, G. L., and A. D. D'Andrea. 2009. How the fanconi anemia pathway guards the genome. *Annu. Rev. Genet.* **43**:223–249.
- Murakawa, Y., et al. 2007. Inhibitors of the proteasome suppress homologous DNA recombination in mammalian cells. *Cancer Res.* **67**:8536–8543.
- Nicassio, F., et al. 2007. Human USP3 is a chromatin modifier required for S phase progression and genome stability. *Curr. Biol.* **17**:1972–1977.
- Nijman, S. M., et al. 2005. The deubiquitinating enzyme USP1 regulates the Fanconi anemia pathway. *Mol. Cell* **17**:331–339.
- Nijman, S. M., et al. 2005. A genomic and functional inventory of deubiquitinating enzymes. *Cell* **123**:773–786.
- Oestergaard, V. H., et al. 2007. Deubiquitination of FANCD2 is required for DNA crosslink repair. *Mol. Cell* **28**:798–809.
- Pace, P., et al. 2010. Ku70 corrupts DNA repair in the absence of the Fanconi anemia pathway. *Science* **329**:219–223.
- Smogorzewska, A., et al. 2010. A genetic screen identifies FAN1, a Fanconi anemia-associated nuclease necessary for DNA interstrand crosslink repair. *Mol. Cell* **39**:36–47.
- Sonoda, E., et al. 1998. Rad51-deficient vertebrate cells accumulate chromosomal breaks prior to cell death. *EMBO J.* **17**:598–608.
- Sowa, M. E., E. J. Bennett, S. P. Gygi, and J. W. Harper. 2009. Defining the human deubiquitinating enzyme interaction landscape. *Cell* **138**:389–403.
- Stewart, G. S., et al. 2009. The RIDDLE syndrome protein mediates a ubiquitin-dependent signaling cascade at sites of DNA damage. *Cell* **136**:420–434.
- Takata, M., et al. 1998. Homologous recombination and non-homologous end-joining pathways of DNA double-strand break repair have overlapping roles in the maintenance of chromosomal integrity in vertebrate cells. *EMBO J.* **17**:5497–5508.
- Wiltshire, T. D., et al. 2010. Sensitivity to poly(ADP-ribose) polymerase (PARP) inhibition identifies ubiquitin-specific peptidase 11 (USP11) as a regulator of DNA double-strand break repair. *J. Biol. Chem.* **285**:14565–14571.
- Zhang, D., K. Zaugg, T. W. Mak, and S. J. Elledge. 2006. A role for the deubiquitinating enzyme USP28 in control of the DNA-damage response. *Cell* **126**:529–542.
- Zhao, G. Y., et al. 2007. A critical role for the ubiquitin-conjugating enzyme Ubc13 in initiating homologous recombination. *Mol. Cell* **25**:663–675.